

Low-loss sharp bends in low contrast polymer hybrid metallic waveguides

M.A. Sefunc*, W. van de Meent, A.R. Coenen, A. Pace, M. Dijkstra, S.M. García-Blanco
Optical Sciences Group, MESA+ Institute for Nanotechnology, University of Twente,
P.O. Box 217, 7500 AE Enschede, The Netherlands

ABSTRACT

Surface plasmons polaritons have drawn significant attention in recent years not only thanks to their capability of confining the field in the dielectric/metal interface, but also thanks to their potential to produce highly efficient thermo-optical or electro-optical devices such as modulators and switches due to the presence of the metal layer amidst the electromagnetic field. However, the high confinement comes at the cost of high propagation losses due to the metal's highly absorptive nature at visible and near-IR wavelengths. In order for plasmonic devices to find a widespread use in integrated optics, an advantage over dielectric waveguides needs to be found that justifies their utilization.

In this work, we present an application in which metallic waveguides perform better than their dielectric counterparts. By adding a thin metallic layer underneath the waveguide core, the total bend losses (dB/90°) are reduced with respect to the bend losses of the equivalent dielectric structure without the metallic layer for a range of radii from 35 μm down to 1 μm. The results show a dramatic reduction of total bend losses in TE-polarization with values as low as 0.02 dB/90° bend for radii between 6 and 13 μm. The mechanism for the reduction of bend losses is the shielding action of the metal layer, which prevents the field to leak into the substrate. In this paper, both detailed theoretical calculations as well as experimental results for SU-8 channel waveguides will be presented.

Keywords: SU-8, optical waveguide, bend waveguide, metal, bend loss

1. INTRODUCTION

Integrated optical devices in polymeric materials have received a significant amount of attention over the last couple of decades thanks to their advantages over other material systems, including low material cost, flexibility and ease of fabrication^{[1][2]}. Polymer materials are compatible with many photonic technologies covering a wide range of refractive index values and exhibiting large transparency window. However, polymer waveguides require large radii of curvature, typically in the order of a few tens of micrometers, to exhibit low propagation loss in bends due to the low refractive index contrast between core and cladding typically obtained in such waveguide architectures^[3].

In this study, we propose the introduction of a thin metallic layer underneath the core of a polymer waveguide to reduce the total bend loss (dB/90°) in sharp bends. Our numerical study shows that the reduction in bend loss with respect to the polymer waveguide without metal layer underneath the core is considerable for radii below 35 μm for transverse electric (TE) mode propagation. For the TE modes, the total bend loss in the metallic waveguide was calculated as low as ~0.02 dB/90°. In the case of TM mode, the total bend loss in the metallic waveguide is lower than that of the dielectric structure for radii ranging from 3 to 10 μm. The experimental characterization results confirm that depositing a thin layer of gold (Au) reduces the losses of sharp bends in polymer (i.e. SU-8) waveguides. This design approach enables the utilization of low-loss polymer waveguides in highly integrated optical circuits, where sharp bends are essential; such as ring resonators with large FSR and optical interconnects.

2. PROPOSED ARCHITECTURE

The waveguide architectures studied in this work are presented in Fig. 1. The proposed configuration corresponds to a dielectric-loaded hybrid metallic waveguide consisting of a polymer core and a thin metal layer underneath that is separated by a thin low refractive index dielectric buffer layer [Fig. 1(a)]. The waveguide core material chosen is the negative-tone epoxy resist, SU-8, although similar results apply to a wide range of architectures exhibiting low refractive

*m.a.sefunc@utwente.nl; phone +31 53 489 2146; fax +31 53 489 3511; os.tnw.utwente.nl

index contrast between substrate and core. In this work, the material of the thin buffer layer is SiO₂ and the metal layer is Au^[4]. The waveguide architecture was built on a Si wafer, which is covered with a sufficiently thick layer of thermal SiO₂ so that the mode is not influenced by the presence of silicon. The dielectric counterpart, the reference structure, does not include any metal layer as shown in Fig. 1(b). The dielectric-loaded hybrid metallic waveguide [Fig. 1(a)] will be referred to as “metallic” in the subsequent sections, whereas the dielectric polymer waveguide [Fig. 1(b)] will be called as “non-metallic”. The refractive indices of the materials employed in this study are given in Table 1 at the wavelength of interest (C-band, $\lambda = 1.55 \mu\text{m}$). The total loss (TL) in a 90° bend of radius R was calculated from the imaginary part of the effective refractive index of the mode with the equation below,

$$TL (dB/90^\circ) = 10 \log_{10}[\text{Im}(n_{\text{eff}})k_o\pi] \tag{1}$$

where n_{eff} is the complex effective refractive index of the guided mode in the bend waveguide and k_o is the wavenumber in vacuum ($k_o = 2\pi/\lambda$). The calculated TL term includes both the radiation loss due to the waveguide curvature (i.e., bend losses) as well as the propagation loss due to absorption in the metal and SU-8 layers. The finite difference (FD) mode calculations were performed in FieldDesigner software of Phoenix Software B.V.

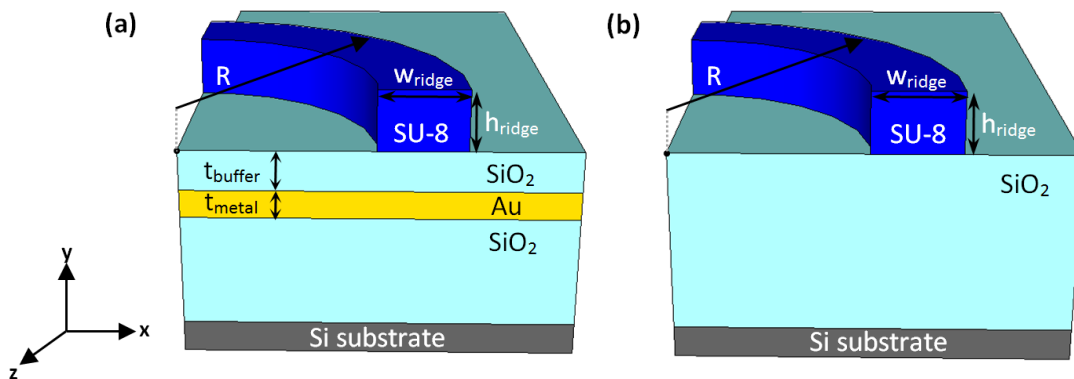


Figure 1. (a) 3-D view of dielectric-loaded hybrid metallic waveguide (“metallic”) and (b) dielectric reference structure (“non-metallic”) considered in this study.

Table 1. Refractive indices of the materials employed in the simulations at the wavelength of 1.55 μm .

	Material Type	Index of Refraction
Under cladding	SiO ₂	1.444
Metal	Au	$0.55 + i*11.5$
Buffer	SiO ₂	1.444
Ridge/Channel	SU-8	$1.57 + i*4.93e-6$
Upper cladding	Air	1

3. RESULTS AND DISCUSSION

The real part of the dominant electric field component for TE (i.e. E_x) and TM (i.e. E_y) modes supported by the “non-metallic” and the “metallic” waveguide architectures are depicted in Figs. 2(a)-(b) and Figs. 2(c)-(d) respectively. The radius of curvature of waveguides in Fig. 2 is 4 μm . The E-field profiles show that the guided mode binds to the outer (right-hand side) rim of the channel, since the light rotates in the direction of the negative x-axis as depicted in Fig. 1. In the non-metallic architecture, the generated leaky waves can be clearly observed and are due to the small radius of curvature of the waveguide. As the curvature is further decreased, the leakage into the substrate increases. This behavior translates into a rapid increase of the bend losses for decreased radii of curvature, as can be observed in Figs. 2(e) and 2(f) for the case “non-metallic”.

The radiated waves due to sharp bending are blocked by the introduction of the thin metallic layer underneath the polymer core. The guided TE mode is pushed towards the channel in the positive y-axis direction [Fig. 2(c)]. Figure 2(e) depicts the total loss per 90° bend for the metallic TE mode in comparison with those of the TE mode of the reference structure. For large radii of curvature, the total loss per 90° bend of the metallic structure rises linearly with increasing radius. The total loss is dominated by the propagation loss, which increases as the length of the waveguide becomes longer. When the radius of curvature decreases below a critical value (i.e. $R \approx 6 \mu\text{m}$), the total loss rises again due to the strong radiation of light in sharp bends. It can be clearly seen in Fig. 2(e) that the introduction of the thin metal layer shifts the optimum radius to a much lower value (i.e. $\sim 6 \mu\text{m}$) than in the non-metallic waveguide (i.e. $\sim 70 \mu\text{m}$). Below a radius of $\sim 35 \mu\text{m}$, the total loss per 90° bend of the metallic structure is smaller than the one of the non-metallic structure. This is particularly interesting for radii between 6 and 13 μm , where calculated losses as low as 0.02 dB/90° [inset of Fig. 2(e)].

The thin metallic layer underneath the polymer channel transforms the photonic TM mode of the non-metallic structure [Fig. 2(b)] into a plasmonic-photonic hybrid mode. Such a hybrid mode is partially coupled to the metal and therefore, leakage to the substrate is prevented [Fig. 2 (d)]. For a narrow range of bend radii from 3 μm to 10 μm , the metallic structure exhibits lower total losses compared to the non-metallic counterpart [inset of Fig. 2(f)]. However, due to the absorption of metal at the wavelength of interest, high propagation losses are observed for increasing radii in which the absorption of metal layer becomes dominant [Fig. 2(f)].

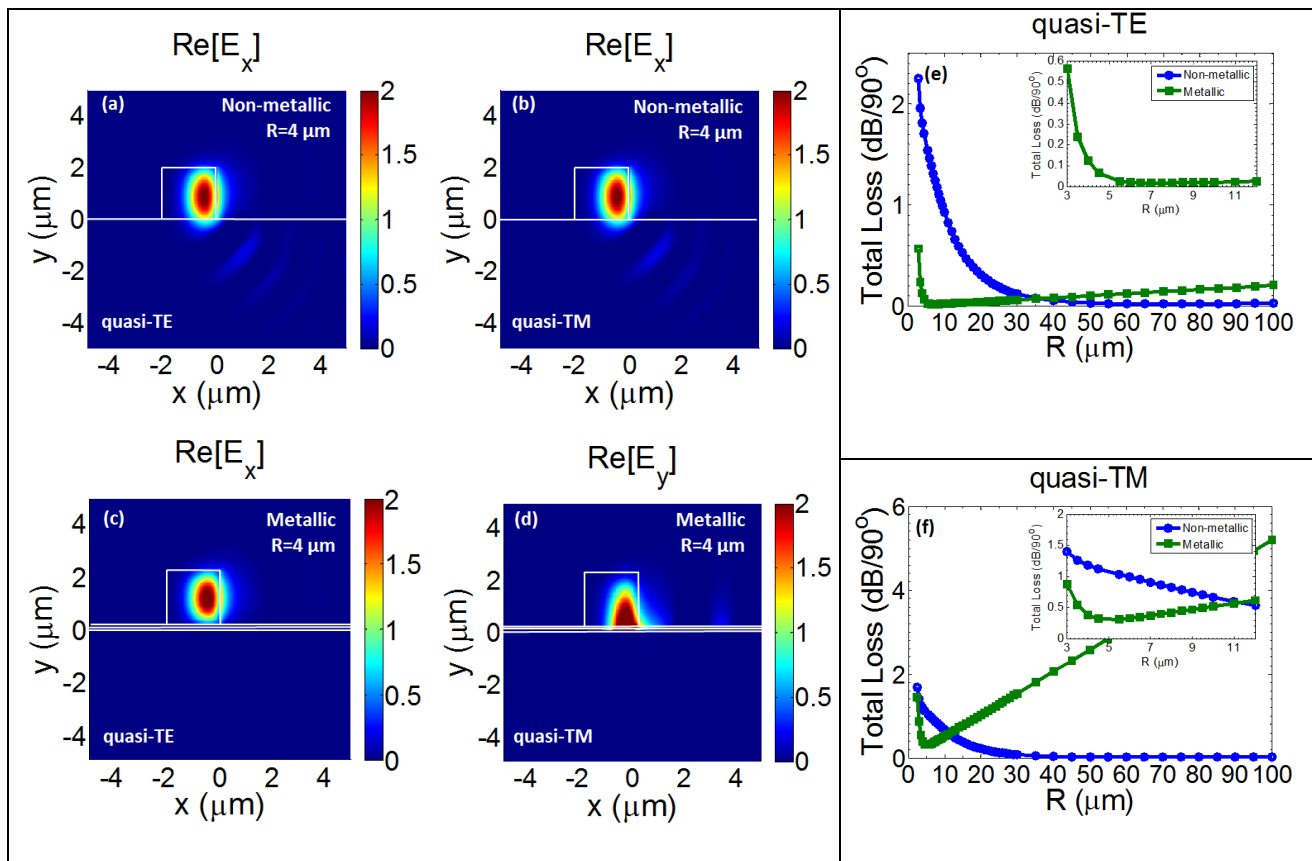


Figure 2. Calculated 2-D mode profiles at $\lambda = 1.55 \mu\text{m}$, $R = 4 \mu\text{m}$ for the non-metallic structures (a-b) with the parameters of $w_{\text{ridge}} = 2 \mu\text{m}$, $h_{\text{ridge}} = 2 \mu\text{m}$ for the (a) TE and (b) TM modes and for the metallic structures (c-d) with the parameters of $w_{\text{ridge}} = 2 \mu\text{m}$, $h_{\text{ridge}} = 2 \mu\text{m}$, $t_{\text{buffer}} = 100 \text{ nm}$ and $t_{\text{metal}} = 50 \text{ nm}$ for the (c) TE and (d) TM modes. Total loss (dB/90°) versus bend radius (R) for metallic and non-metallic structures for (e) TE and (f) TM modes. The insets are a zoom of the corresponding loss plots in the region of interest.

3.1 Fabrication of SU-8 waveguides

Metallic and non-metallic waveguides with various number of bends were fabricated to understand how the metal layer improves the system losses in a polymer waveguide. For the comparison, two identical set of waveguides on different substrates; one with a gold layer underneath the bends [Fig. 3 (a)] and the other without any metal [Fig. 3 (b)], were fabricated.

The fabrication of the metallic waveguides can be summarized in the following three main steps: (1) patterning of the gold layer; (2) depositing the SiO₂ buffer layer; and (3) patterning of the waveguides on SU-8 resist. A silicon wafer with pre-grown 8 micrometer thick thermal SiO₂ layer on top as the substrate was utilized. After cleaning the substrate with standard wafer cleaning procedure, a positive photoresist (OIR 907/17) was spin coated on the wafer. The resist was patterned using standard UV-photolithography to define the gold layer, which will be only located underneath the bend sections of the waveguides. A 50 nm thick gold layer was evaporated on the wafer and the leftover positive resist was lifted-off. A 100 nm thick amorphous SiO₂ buffer layer deposited using electron beam evaporation method (Balzers BAK 600). SU-8 resist was spin-coated on the wafer with the thickness of 2 micrometers. The last step was the patterning of the SU-8 resist to define the channel SU-8 waveguides with 2 micrometer width. For the fabrication of the dielectric counterpart, the non-metallic waveguides, the same process flow was followed except the steps for of the lift-off patterning of the gold layer.

Each SU-8 waveguide consists of a pure dielectric input and output section attached to a sinusoidal bend. The input sections of the waveguides include a taper with a taper angle of 0.5° to achieve improved in-coupling of light.

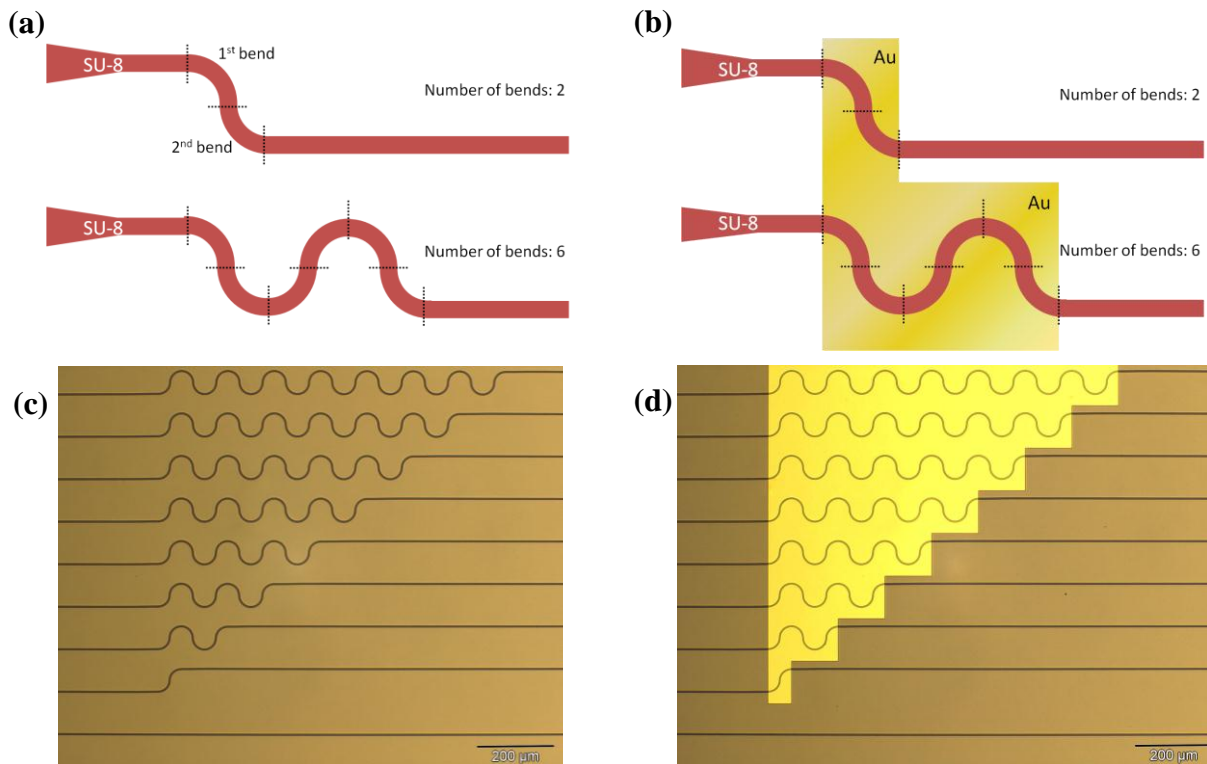


Figure 3. Schematic of (a) non-metallic and (b) metallic waveguides with different number of 90° bends (N): 2 and 6 bends with tapers (The sketches are not drawn in scale). Microscope image of fabricated (c) non-metallic and (d) metallic waveguide with 30 micron radius of curvature including various number of bends (N): 0, 2, 6, 10, 14, 18, 22, 26, 30 bends.

3.2 Characterization results of metallic and non-metallic SU-8 waveguides

In this comparative study, the fabricated metallic and non-metallic waveguides with different number of bends were characterized by measuring the power of the transmitted light through those waveguides. A schematic of the

characterization setup is shown in Fig. 4. A semiconductor laser diode emitting at the wavelength of 1550 nm with a pigtailed polarization-maintaining (PM) fiber was used as the light source in the measurements. The current of the laser diode was kept constant in all the measurements. The polarization of the input light was set to TE. In the input stage, the divergent beam coming from the fiber tip was collimated with an objective lens with 4X magnification. The collimated beam was then focused to the waveguide using another objective lens with 10X magnification. We used an objective lens on the output stage to focus the output light coming from the waveguide end-facet on the IR power detector. To optimize the coupling at each measurement, the position of the input and output stages were tuned until the output power was maximized. This optimization procedure enabled to obtain reliable measurements that were reproducible within an error margin of 10%.

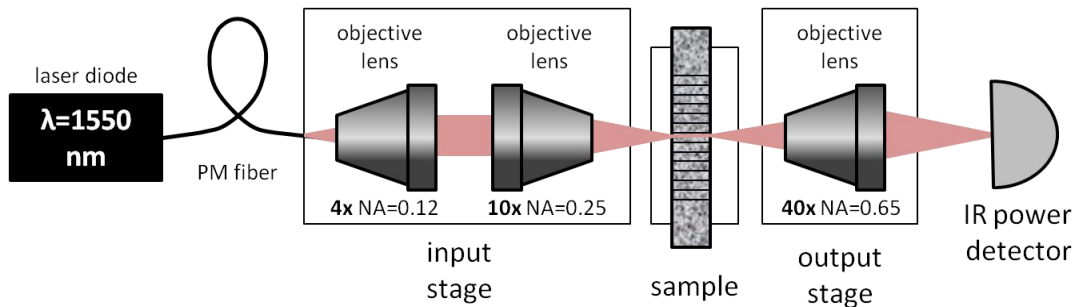


Figure 4. Experimental setup for measuring transmitted light through the waveguides.

The fabricated waveguides include connection points, including dielectric straight to metallic bend in the metallic waveguides and dielectric straight to dielectric bend in non-metallic waveguides. At those connections, the light radiates due to mismatch in the mode profiles. The transition losses strongly depend on the particular waveguide parameters such as the architecture of waveguide, radii of curvature of the bends and the polarization of the light. The mode overlap calculations for the fabricated structure indicate that embodying a thin metal layer also reduces the transition losses by keeping the mode in the core of the waveguide. Consequently, the mode overlap increases at the connection points.

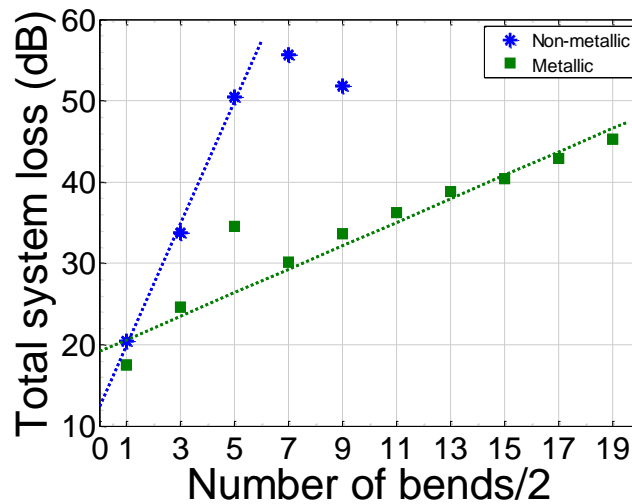


Figure 5. Total system loss versus numbers of bends divided by 2 ($N/2$) for metallic and non-metallic SU-8 waveguides with $R = 4 \mu\text{m}$ for TE polarization. A linear fit was defined for each dataset. The non-metallic measurements with 14 and 18 bends were not included in linear fitting process since the measured output power was in the noise regime. Damages on the waveguide surface and the variation on the quality of the end facets induce extra losses that might cause fluctuations in output power measurements, leading to unexpectedly high losses: the system loss for the metallic waveguide with 10 bends is much higher than expected, which is due to damages on the waveguide surface.

In this study, non-metallic and metallic SU-8 waveguides with radius of curvature of 4 micrometers with various numbers of bends were characterized. As shown in Fig. 3, the metallic and non-metallic waveguides are identical except

for the gold layer in metallic waveguide set. Fig. 5 shows the total system loss (in dB) versus number of bends in the waveguide as defined in Figs. 3(a) and (b). The total system loss was calculated as $TSL = 10 \cdot \log_{10}(P_{out}/P_{in})$ where P_{out} is the measured output power and P_{in} is the input power measured just after the input stage of the setup.

The total system loss depends on the number of bends in the waveguide and increases significantly by increasing number of bends. The slope of the fits represents the sum of two total bend loss and a bend-to-bend loss; $d(TSL)/d(N/2) = 2 \cdot \text{bend loss} + \text{bend-to-bend loss}$. The output power for the non-metallic waveguides decreases very quickly to noise regime ($\sim 0.010 \mu\text{W}$) by increasing number of bends due to strong loss in the waveguide. Therefore, output power measurements for non-metallic waveguides with more than 18 bends were not taken. As depicted in Fig 5, the total system loss of the non-metallic waveguides increases quicker than of the metallic waveguides. This can be interpreted as the combination of total bend loss and bend-to-bend loss in metallic waveguides, ~ 1.44 dB, are lower compared to their non-metallic counterpart, ~ 7.5 dB, for the same input power. We are currently working on the fabrication of new structures that will permit us to differentiate between the total bend loss and bend-to-bend loss.

4. CONCLUSION

In this work, we proposed and demonstrated that introducing a thin metal layer underneath the core of a polymer waveguide permits to reduce the losses of sharp bends in SU-8 waveguide for TE polarization. The FD mode calculations indicate more than 10-fold reduction of the bend losses with respect to the dielectric structure for radii below $\sim 35 \mu\text{m}$ for TE modes. The characterization results confirm that depositing a thin layer of gold reduces the losses in sharp bends in SU-8 waveguides. The approach considered in this paper promise to improve the performance of polymer waveguides in large-scale photonic integration where sharply bent waveguides with radii of a few micrometers are essential to shrink the footprint of photonic circuitry.

REFERENCES

- [1] Eldada, L. and Shacklette, L.W., "Advances in polymer integrated optics," IEEE J. Sel. Top. Quantum Electron. 6(1), 54-68 (2000).
- [2] Ma, H., Jen, A.K.Y. and Dalton, L.R., "Polymer-based optical waveguides: materials, processing and devices," Adv. Mater. 14(19), 1339-1365 (2002).
- [3] Sefunc, M. A., Pollnau, M. and García-Blanco, S.M., "Low-loss sharp bends in polymer waveguides enabled by the introduction of a thin metal layer," Opt. Express 21(24), 29808-29817 (2013).
- [4] Palik, E.D., "Handbook of Optical Constants of Solids," Academic Press (1985).